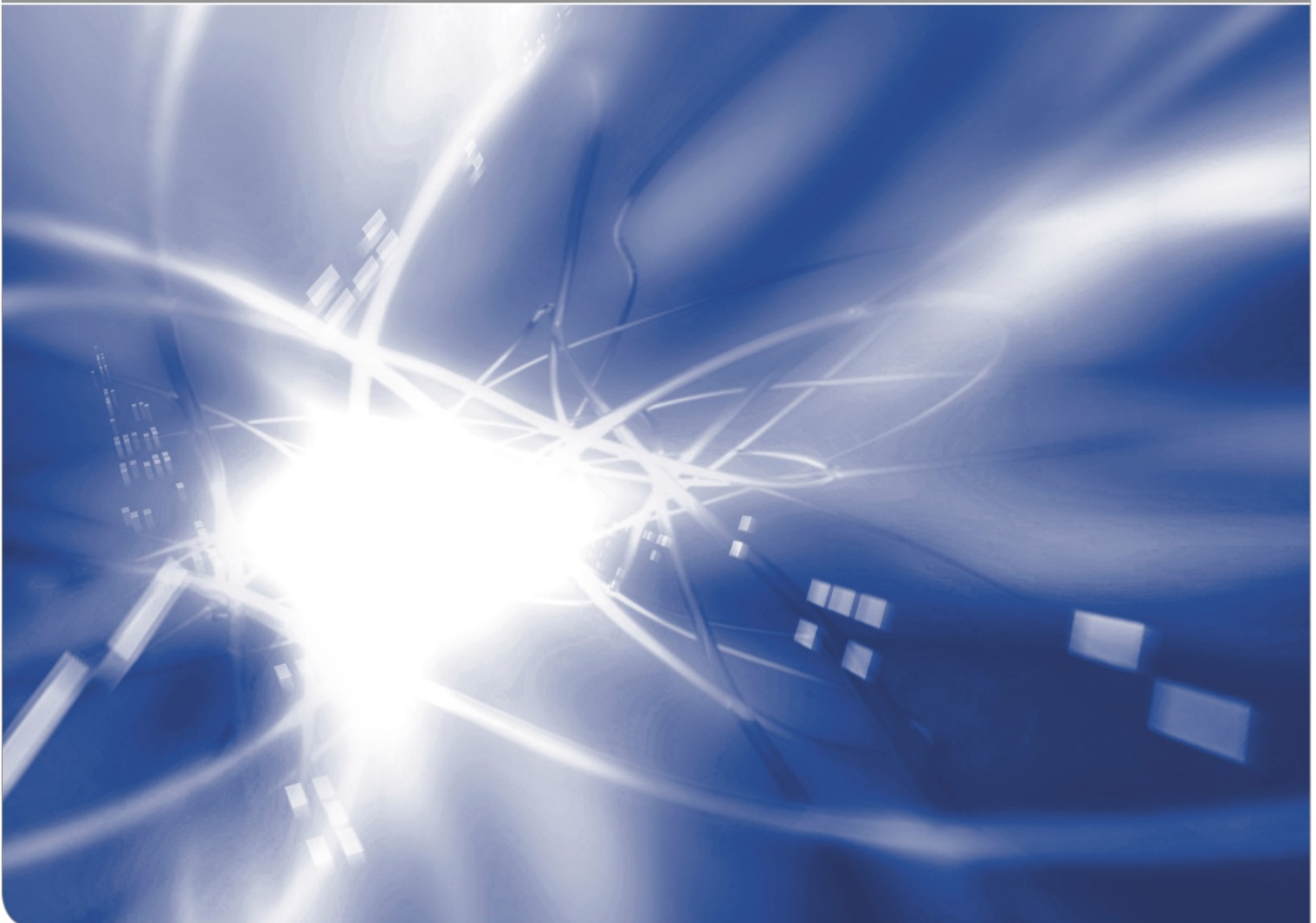


# Proceedings of the 1st Workshop on Proximity Perception in Robotics at IROS 2018, Madrid, Spain

Edited by

Stefan Escalda Navarro<sup>1</sup>, Stephan Mühlbacher-Karrer<sup>2</sup>,  
Hosam Alagi<sup>3</sup>, Björn Hein<sup>3</sup> and Hubert Zangl<sup>4</sup>

October, 1, 2018 Madrid, Spain.  
IEEE/RSJ International Conference on Intelligent Robots and Systems



<sup>1</sup> Inra Lille – Nord Europe

<sup>2</sup> JOANNEUM RESEARCH ROBOTICS

<sup>3</sup> Intelligent Process Automation and Robotics Lab (IPR)

<sup>4</sup> Alpen-Adria Universität Klagenfurt

Inra Lille – Nord Europe  
40 Avenue Halley  
59650, Villeneuve d'Ascq, France  
[www.hautsdefrance.inra.fr](http://www.hautsdefrance.inra.fr)

JOANNEUM RESEARCH ROBOTICS  
Leonhardstrasse 59  
8010 Graz, Austria  
[www.joanneum.at](http://www.joanneum.at)

Intelligent Process Automation and Robotics Lab (IPR)  
Engler-Bunte-Ring 8  
76131 Karlsruhe, Germany  
[www.ipr.kit.edu](http://www.ipr.kit.edu)

Alpen-Adria-Universität Klagenfurt  
Universitätsstraße 65-67  
9020 Klagenfurt am Wörthersee, Austria  
[www.aau.at](http://www.aau.at)

### Impressum

Karlsruher Institut für Technologie (KIT)  
[www.kit.edu](http://www.kit.edu)



This work is licensed under a Creative Commons Attribution-NonCommercial-NoDerivatives 4.0 International License: <https://creativecommons.org/licenses/by-nc-nd/4.0/>  
2018

# Introduction

In this workshop the topic of Proximity Perception and its community was brought into a spotlight. The goal of the workshop was to establish networks and a vivid community in Proximity Perception and open the topic to the wider robotics community, as we expect that Proximity Perception technologies will play an essential role for service and industrial robotics as well as for safe human-robot collaboration and compliant robotics applications in the near future.

These proceedings contain the papers accepted and presented during the poster session of the workshop.

## Talks held at the workshop:

A unified Sensor for Pre-Touch, Touch and Post-Touch Force Measurement

Joshua R. Smith, University of Washington

Making the Best of Pretouch

Gordon Cheng, Technical University of Munich

Biomimetic Tactile Sensing and Haptics

Nathan Lepora, University of Bristol

Reactive Control for High-Speed Grasping using Optical Proximity Sensors

Keisuke Koyama, The University of Tokyo

Tactile Servoing Algorithms for Manipulation and Object Exploration

Robert Haschke, Bielefeld University

Ultra Short Range Radar for Human Machine Interaction

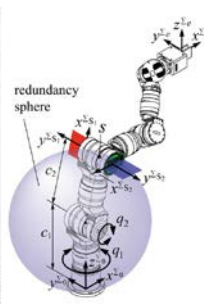
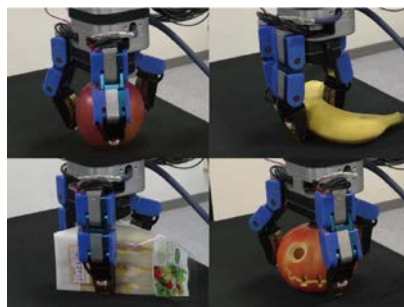
Matthias Brandl, Infineon Technologies

Near Field Tomography in Proximity Perception

Hubert Zangl, Alpen-Adria-Universität

Sensor Technology and Algorithms for Flexible Proximity and Tactile Perception

Björn Hein, Karlsruhe Institute of Technology



For more information,  
please visit the  
workshop website.

[proxelsandtaxels.org](http://proxelsandtaxels.org)



# Versatile distance measurement between robot and human key points using RGB-D sensors for safe HRI

Petr Švarný, Zdenek Straka, and Matej Hoffmann<sup>1</sup>

**Abstract**—The safety of collaborative robots’ and human interaction can be guaranteed in two main ways: (i) power and force limiting and (ii) speed and separation monitoring. We present a framework that realises separation distance monitoring between a robot and a human operator based on key point pair-wise evaluation. We show preliminary results using a setup with a Nao humanoid robot and a RealSense RGB-D sensor and employing OpenPose human skeleton estimation algorithm, and work in progress on a KUKA LBR iiwa platform.

## I. INTRODUCTION

Collaborative robots (cobots) need to dynamically adapt to interactions with people to guarantee safety at every moment. The technical specification [1] introduces *Speed and Separation Monitoring (SSM)* as a requirement to ensure safety. SSM demands that a *protective separation distance*,  $S_p$ , needs to be maintained at all times between the operator and robot. When the distance decreases below  $S_p$ , the robot stops [2]. When  $S_p$  is approached, the robot can lower its speed to be able to stop in the case of intrusion. The industry standard is to use different levels of safety zones guarded by light curtains or safety-rated scanners.

We present an SSM approach that combines transparency and versatility. The separation distance is assessed pair-wise for all key points on the robot and the human body and can be selectively modified to account for various interaction scenarios.

## II. RELATED WORK

The safety standards related to cobots are [1], [2] and a survey of the aspects of physical Human-Robot interaction (pHRI) can be found in [3]. An analysis of appropriate metrics to measure SSM is in [4]. A functional solution for safe pHRI according to SSM requirements involves (i) sensing of the human operators’ as well as robot’s positions and speeds, (ii) a suitable representation of the corresponding separation distances and (iii) appropriate responses of the machine.

Zone scanners as used in industry are safe but very inflexible and prevent most collaborative activities, since

\*This work was supported in part by the Czech Science Foundation under Project GA17-15697Y and by the Czech Technical University in Prague, grant No. SGS18/138/OHK3/2T/13.

<sup>1</sup> Department of Cybernetics, Faculty of Electrical Engineering, Czech Technical University in Prague. {petr.svarny, zdenek.straka, matej.hoffmann}, @fel.cvut.cz

their resolution is essentially only binary (for every zone): either a human entered the zone or not. Progress in this area may be facilitated by (i) compact and affordable RGB-D sensors (like Kinect) and (ii) convolutional neural networks for human key point extraction from camera images [5], [6]—that together provide a more detailed picture about the human’s activities in the robot’s proximity.

Relative distances between human and robot key points need to be evaluated (see Flacco et al. [7] for a comparison of approaches). The approach is often “robot-centred” in the sense that the collision primitives are centred on the robot body and possibly dynamically shaped based on the current robot velocity [8], [9], [10], [11]. Even the biologically inspired approach to “peripersonal space” representation [12], [13] is robot-centred. Liu and Tomizuka [14] present a comprehensive framework that includes avoidance manoeuvres of the robot and task execution while preserving safety constraints. However, it is not clear whether this framework could pass a risk assessment according to [1], [2].

We propose an SSM framework to enhance the safety of pHRI. It treats robot and human key points equally and uses Euclidean distance in Cartesian space to evaluate all safety thresholds. Velocities, reaction and stopping times, and uncertainties can all be made part of our framework following [2]. Unique to our approach, the representation is maximally transparent as it does not contain any black-box component. However, at the same time, additional features—like the different sensitivity of human body parts or tools modifying the robot’s safety—can be easily incorporated. Also, the use of key points instead of other representations supports the transparency and interpretability of the framework.

## III. MATERIALS AND METHODS

The framework uses extracted human and robot key points. The relative distances are assessed and fed into the robot controller to generate the appropriate response.

### A. Human key point estimation

We used a currently commercially available RGB-D camera RealSense SR300 that provides a Colour Image Aligned to the Depth image Stream (CADS) and a point cloud stream (PCS), also depth image aligned. We use PyRealSense to combine these streams. The CADS image is processed by PyOpenPose [5] to calculate the estimated human key point coordinates. Their 3D location is obtained through pairing with the PCS. All our image operations use OpenCV3 [15].

The key points are transformed into the robot’s frame of reference by affine transforms with parameters from a pre-experiment calibration.

### B. Robot key points

A Nao humanoid robot (V3+) was used in the preliminary experiments. Its key points were on the left end-effector, forearm, and elbow. We used forward kinematics with current joint encoder values as input to get the 3D position of these key points. A Kuka LBR iiwa is the goal platform for the experiment.

### C. Separation distance representation

The *protective separation distance*  $S_p$  [2] needs to be maintained between any human and robot part, such that the human will never collide with a moving machine. Its value is given as a sum of different contributors like reaction times, detection uncertainties etc. For more detail, see Section 5.5.4.2.2 of [2]. With  $S_p$  as a baseline, we extend it with additional terms.

First, we want to account for “modulation” on the part of the human to grant larger distance from specific body parts (e.g. head) and on the part of the robot-like when carrying a sharp tool. Adding these distance offsets  $\mathbf{r}_s$ ,  $\mathbf{h}_s$  gives rise to a *guaranteed minimal separation distance*  $S_g$ . The methodology for determining the exact values of these offsets is currently in development.

Second, as only distances between key points will be evaluated, but separation distance between any body parts needs to be maintained, we add compensation coefficients,  $\mathbf{h}_{compen}$  and  $\mathbf{r}_{compen}$  (see Section III-D below), giving the *key point separation distance*  $S_d$ —the quantity that will be monitored between any key point pairs.

Therefore  $S_d$  is in the form of a matrix of  $S_d^{i,j}$  between two given key points  $i, j$  (see Section IV).

### D. Key point compensation coefficients

Using a discrete distribution of key points does not take the full volume of the bodies into account. The compensation coefficients  $\mathbf{h}_{compen}$  and  $\mathbf{r}_{compen}$  allow us to guarantee  $S_g$  even with a discrete key point distribution.

Every part of the body is assigned to its nearest key point. The maximal distance over all of its assigned volume is selected as the compensation coefficient for the given key point—thereby always guaranteeing  $S_g$ . See Fig. 3. The current autonomous finding of these coefficients uses the robots URDF model to approximate the maximal distances between the key point and the assigned volume.

### E. Robot control

We used PyNaoqi to control the Nao robot and ROS and the FRI interface to control the KUKA LBR iiwa robot. The robot was moving his end-effector periodically back and forth on a fixed path when undisturbed. The robot stopped when the  $S_d^{i,j}$  threshold was exceeded. The robot resumed

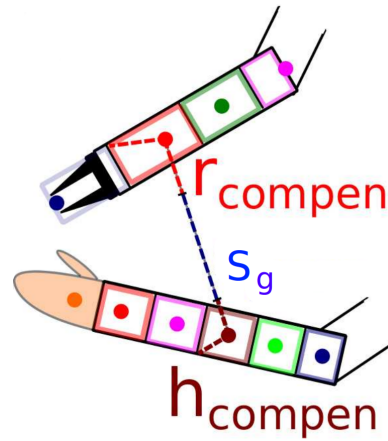


Fig. 1: Separation distance calculation between robot and human key points.

operation upon “obstruction” removal. Also, we defined a reduced speed distance: when  $S_d^{i,j(reduced)}$  for any key point pair was exceeded, the robot reduced its speed to half.

### F. HRI setup

The robot was in a fixed position to the camera that captured the robot’s workspace. The threshold  $S_p$  is determined based on [2] for the KUKA or chosen arbitrarily in the case of the non-harmful NAO.

The compensation values accounting for key point density (Section III-D) were determined by measuring the distances between key points. Only upper body key points were taken into consideration for the human operator. We call the human head the set of key points of the nose, neck, eyes and ears. In both, human and robot case, the compensation coefficient values were sagittal symmetric, and thus we list key points pairs only once.

## IV. EXPERIMENTAL VALIDATION

We tested the framework with an SSM scenario between the NAO robot and a human with specific separation values for the head of the human. Distances between all human and robot key points were evaluated simultaneously online. However, for clarity, we present only the interaction of the robot end-effector with two human key points (the right wrist and the nose) in the plots below.

The baseline protective separation distance was set to  $S_p = 0.05m$  and the one that brings the robot to reduced speed regime  $S_p(reduced) = 0.20m$ . The  $\mathbf{h}_s$  for the head key points was enlarged by  $0.15m$ . This lead to the robot’s higher sensitivity to situations when the human operator approached the robot with his head, as shown in Fig. 2.

We see the reaction of the robot to the wrist key point. Later, we see that the robot reacts to the proximity of the nose key point already at a greater distance. Notice the different reactions of the robot (shown by the different shading) for similar distances of the two key points.

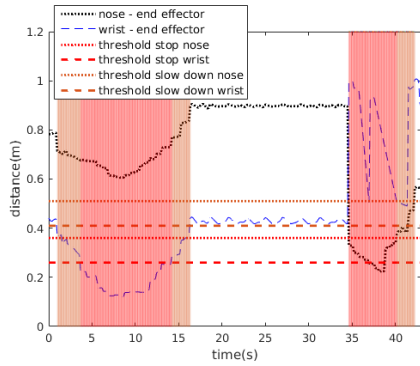


Fig. 2: Head and body discrimination: A higher separation threshold for the human head region w.r.t. Nao robot’s end-effector. Yellow areas mark the robot’s slower movement and red areas mark when he stopped.

Robot \ Human	$S_d(\text{reduced})$	Wrist
<b>End effector</b>	<b>Nose</b> 0.51m	0.41m

Robot \ Human	$S_d$	Wrist
<b>End effector</b>	<b>Nose</b> 0.36m	0.26m

TABLE I: Head and body discrimination: Separation matrix for key point pairs from Fig. 2.

## V. CURRENT WORK AND OUTLOOK

The presented framework is general enough to be applied to any collaborative scenario. We currently modify the representation to fit the KUKA LBR iiwa robot (Fig. 3). As opposed to the NAO robot, this platform is “collaborative”, but its dimensions and maximum speed make appropriate risk assessment necessary.

## VI. DISCUSSION AND CONCLUSION

We presented a framework that realises speed and separation monitoring between a robot and a human operator in a versatile and transparent fashion.

OpenPose provides confidence values with every key point estimated. Confidence values would allow to alleviate problems with possible misdetections and make the framework more robust. After validating the framework on an industrial robot, this is our next goal.

Currently, there are no commercially available safety-rated RGB-D sensors suitable for such a framework. If our framework is used in industrial settings, safety-rated devices similar to those for zone monitoring that would provide at least 3D object coordinates would be needed.

## REFERENCES

[1] “ISO 10218 Robots and robotic devices – Safety requirements for industrial robots,” International Organization for Standardization, Geneva, CH, Standard, 2011.  
[2] “ISO/TS 15066 Robots and robotic devices – Collaborative robots,” International Organization for Standardization, Geneva, CH, Standard, 2016.

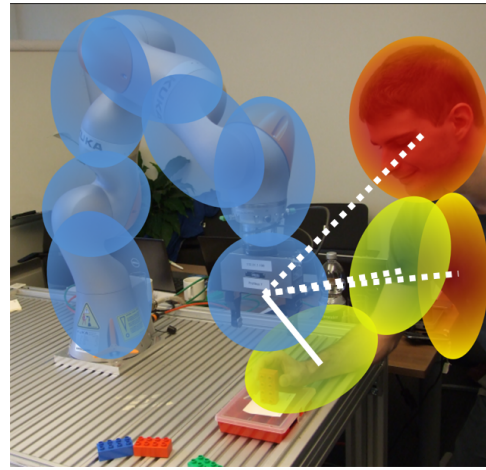


Fig. 3: Preliminary representation of Kuka end-effector and human key point pairs. Ellipses approximate the key point compensation coefficient areas.

[3] S. Haddadin and E. Croft, “Physical human-robot interaction,” in *Springer Handbook of Robotics*, 2nd ed., B. Siciliano and O. Khatib, Eds. Springer, 2016, pp. 1835–1874.  
[4] J. A. Marvel, “Performance metrics of speed and separation monitoring in shared workspaces,” *IEEE Transactions on Automation Science and Engineering*, vol. 10, no. 2, pp. 405–414, 2013.  
[5] Z. Cao, T. Simon, S.-E. Wei, and Y. Sheikh, “Realtime multi-person 2d pose estimation using part affinity fields,” in *CVPR*, vol. 1, no. 2, 2017, p. 7.  
[6] E. Insafutdinov, L. Pishchulin, B. Andres, M. Andriluka, and B. Schiele, “Deepcruc: A deeper, stronger, and faster multi-person pose estimation model,” in *European Conference on Computer Vision*. Springer, 2016, pp. 34–50.  
[7] F. Flacco, T. Kroeger, A. De Luca, and O. Khatib, “A depth space approach for evaluating distance to objects,” *Journal of Intelligent & Robotic Systems*, vol. 80, p. 7, 2015.  
[8] B. Lacevic and P. Rocco, “Kinetostatic danger field—a novel safety assessment for human-robot interaction,” in *Intelligent Robots and Systems (IROS), 2010 IEEE/RSJ International Conference on*. IEEE, 2010, pp. 2169–2174.  
[9] V. Magnanimo, S. Walther, L. Tecchia, C. Natale, and T. Guhl, “Safeguarding a mobile manipulator using dynamic safety fields,” in *Intelligent Robots and Systems (IROS), 2016 IEEE/RSJ International Conference on*. IEEE, 2016, pp. 2972–2977.  
[10] M. P. Polverini, A. M. Zanchettin, and P. Rocco, “A computationally efficient safety assessment for collaborative robotics applications,” *Robotics and Computer-Integrated Manufacturing*, vol. 46, pp. 25–37, 2017.  
[11] A. M. Zanchettin, N. M. Ceriani, P. Rocco, H. Ding, and B. Matthias, “Safety in human-robot collaborative manufacturing environments: Metrics and control,” *IEEE Transactions on Automation Science and Engineering*, vol. 13, no. 2, pp. 882–893, 2016.  
[12] A. Roncone, M. Hoffmann, U. Pattacini, L. Fadiga, and G. Metta, “Peripersonal space and margin of safety around the body: learning tactile-visual associations in a humanoid robot with artificial skin,” *PLoS ONE*, vol. 11, no. 10, p. e0163713, 2016.  
[13] D. H. P. Nguyen, M. Hoffmann, A. Roncone, U. Pattacini, and G. Metta, “Compact real-time avoidance on a humanoid robot for human-robot interaction,” in *Human-Robot Interaction, HRI 18: 2018 ACM/IEEE International Conference on*. IEEE, March 58, 2018, p. 9.  
[14] C. Liu and M. Tomizuka, “Algorithmic safety measures for intelligent industrial co-robots,” in *Robotics and Automation (ICRA), 2016 IEEE International Conference on*. IEEE, 2016, pp. 3095–3102.  
[15] G. Bradski, “The OpenCV Library,” *Dr. Dobbs’s Journal of Software Tools*, 2000.

# A New Capacitive Proximity Sensor for Detecting Ground-Isolated Objects

Yitao Ding<sup>1</sup> and Ulrike Thomas<sup>1</sup>

**Abstract**—In this work, we provide a new measurement method for detecting ground-isolated objects with capacitive sensors. Capacitive sensors find use in sensor skins for safety applications in robotics, where they serve as proximity sensors for proximity servoing. The sensors measure the electric current caused by the capacitive coupling and changing electric field between the sensor electrode and the target. However, these sensors require a return path for the current back to the sensor in order to provide a reference potential, otherwise the targets are electrically floating and not detectable. Our approach allows us to avoid this return path by creating a virtual reference potential in the target with differential signals. We provide experimental results to show the effectiveness of our method compared to state-of-the-art measurement methods.

## I. INTRODUCTION AND APPROACH

Proximity servoing is a growing field of research involving perception, motion planning and sensor technology. The technology, with the capability of near field monitoring, offers new possibilities in terms of flexibility and safety of robots [1]. It enables the exploration of the robot's environment from the robot's point of view with proximity sensors attached on the robot's surface. Compared to external camera-based solutions, these sensor signals are not restricted by occlusion and can be incorporated directly into the motion controller to avoid obstacles [2].

In terms of sensor technology, capacitive sensors find use in sensor skins for proximity sensing [3]. In this paper, we present a new capacitive sensing method for detecting ground-isolated objects [4]. Capacitive proximity sensors measure the projected capacitance formed between the sensor's electrode and the target. Common measurement methods are either based on self capacitance (Fig. 1a) or mutual capacitance (Fig. 1b). Both methods require a return path of the current for a correct reference potential. The self capacitance method relies on the coupling between the target and the environment ground. However, the coupling to the environment is often unknown and is subject to many variables. The return path can be either affected by impedance through the target  $Z'_O$ , and therefore also the contact point of the return path, the size of the object (capacitive coupling), and whether an object is actively grounded (e.g. by wire connection). With the self capacitance method, an isolated object without return path is electrically floating

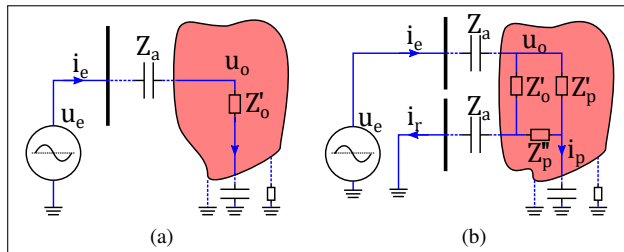


Fig. 1: Projected capacitance measurement methods: 1a) self capacitance, 1b) mutual capacitance.

and is undetectable for the sensor. The mutual capacitance measurement method provides a solution with a second ground electrode as a return path. By this, floating targets are detectable but currents through other paths (leakage current) are still affecting the measurement with less influence compared to the self capacitance method. The authors in [5] provide an estimation approach for the leakage current from data gained from consecutively measuring in self and mutual capacitance mode. The leakage current information is relevant for electrical capacitance tomography. But still the leakage current depends heavily on the materials in the return path and does not allow a precise measurement of the target's material impedance in a spatial limited area.

Our solution (Fig. 2) cancels out the leakage current by actively driving the ground electrode of the mutual capacitance method with a differential signal from the measurement electrode. This allows local capacitive measurements that are unaffected by leakage currents. The leakage current information is lost, with a gain in robustness and reliability for proximity detection while signal acquisition and processing times are reduced. This method is easily implementable in already existing system designs based on mutual capacitance measurement by adding an inverting opamp to the system. Our approach assumes that both electrode stages are equal and requires a symmetric design of both stages with respect to components and electrode area. When these requirements are satisfied, then a virtual ground is created within the target independent of the targets actual ground state.

## II. SYSTEM DESCRIPTION

This section describes our sensor design, which is based on the mutual capacitance sensor presented in [6] with a modification of the ground electrode.

The sensors are (40 mm×40 mm) in size. As presented in Fig 2, we use an unbiased sine signal  $u_e$  as source

<sup>1</sup>All authors are with the Lab of Robotics and Human-Machine-Interaction, Chemnitz University of Technology, 09126 Chemnitz, Germany. Emails: {yitao.ding, ulrike.thomas}@etit.tu-chemnitz.de

with a frequency range of 10 kHz to 300 kHz. An inverting amplifier creates a differential signal  $-u_e$ , which is referred as negative stage in this paper. This amplifier has high bandwidth to keep phase-shifting at minimum and both stages symmetric. Since we measure the electrode current with the measurement resistor  $R_{pm}$  an equal resistor  $R_{nm}$  is added to the negative stage also for symmetry. Both stages are then connected to equally dimensioned (17 mm  $\times$  40 mm) electrodes with shielding electrodes on the backside. A microcontroller samples the electrode current through  $R_{pm}$  with an instrumentation amplifier, and the transmission voltage  $u_e$ .

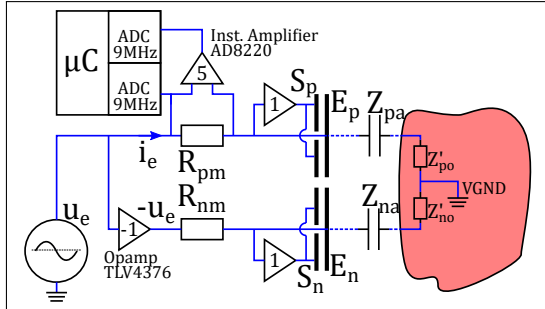


Fig. 2: Schematic of the analog front-end. Creation of a virtual ground within the target with a second differential signal.

### III. EXPERIMENTAL RESULTS

In this section we perform six different measurements by comparing the self capacitance, mutual capacitance, and our proposed differential method with and without a return path (RP). The target is a highly conductive aluminum plate placed on a thick isolating wooden plate. The measurement frequency is 100 kHz with a  $V_{pp}$  of 2.5 V. We calculate the absolute impedance  $Z$  (antiproportional to the capacity) from the sensor's absolute excitation voltage  $\hat{u}_e$  and absolute electrode current  $\hat{i}_e$  at distances ranging from 0.2 mm to 10 mm. As shown in [6], these values can be calculated with  $\hat{u}_e = \sqrt{2 \cdot \langle u_e, u_e \rangle}$  and  $\hat{i}_e = \sqrt{2 \cdot \langle i_e, i_e \rangle}$ .

The measurements in Fig. 3 show that the self capacitance and the mutual capacitance method perform similarly at targets with return path (solid green/blue lines). The lower impedance in the mutual capacitance method is caused by the stronger parasitic capacitance of the second ground electrode on the sensor. However, targets that are isolated from the sensor disturb the signal with an increase of impedance (dotted green/blue lines). The target can still be detected due to the capacitive coupling to the environment. The mutual capacitance method is less affected at close range, because the target acts as permittivity between the measurement electrode and the ground electrode. With increasing ranges the capacitive coupling between both electrodes decreases which results in a similar disturbed impedance as the self capacitance method.

Finally, isolated targets do not disturb measurements from the proposed differential method (red lines). Both lines are

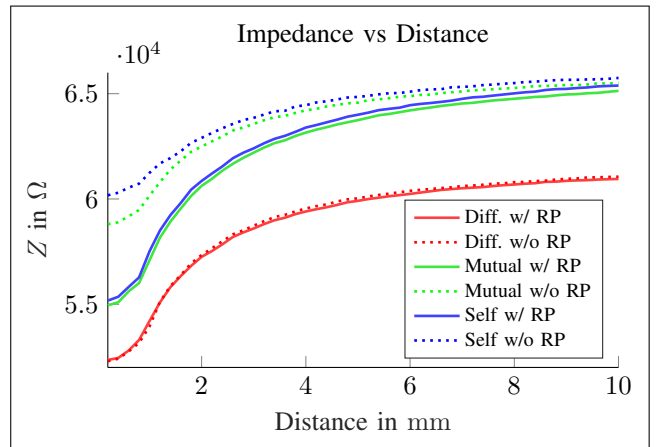


Fig. 3: Measurement of impedance at distances ranging from 0.2 mm to 10 mm. Dotted lines represent an isolated target without return path, whereas solid lines represent targets with return path.

similar, which is the goal of our approach. The second differential electrode causes an overall decrease of the impedance with its stronger parasitic capacitive effect, which can be compensated through calibration as shown in [6].

### IV. CONCLUSIONS

Our proposed differential measurement method for capacitive sensors shows promising results of detecting targets that are ground-isolated and which do not provide a return path for the current. With this in mind, sensors can be designed completely isolated from the environmental ground, e.g. with battery operation. Further external disturbances, such as 50/60 Hz mains noise, can be suppressed. Our method also provides an important contribution towards safe human-robot collaboration applications based on capacitive proximity skins, where a reliable detection of obstacles is essential.

### REFERENCES

- [1] Robert Bosch Manufacturing Solutions GmbH, *APAS Assistant - Contact-Free Human-Robot Collaboration*, [https://www.bosch-apas.com/media/en/apas/downloads/2017\\_12\\_01\\_apas\\_assistant\\_doppelseite\\_de.pdf](https://www.bosch-apas.com/media/en/apas/downloads/2017_12_01_apas_assistant_doppelseite_de.pdf), 2018, online: accessed 7-August-2018.
- [2] T. Schlegl, T. Kröger, A. Gaschler, O. Khatib, and H. Zangl, "Virtual whiskers — highly responsive robot collision avoidance," in *2013 IEEE/RSJ International Conference on Intelligent Robots and Systems*, Nov 2013, pp. 5373–5379.
- [3] H. Alagi, S. E. Navarro, M. Mende, and B. Hein, "A versatile and modular capacitive tactile proximity sensor," in *2016 IEEE Haptics Symposium (HAPTICS)*, April 2016, pp. 290–296.
- [4] Y. Ding and U. Thomas, *Einrichtung zur Bestimmung der elektrischen Kapazität*, Patent applied: AKZ 102018003268.0, submitted: 19-April-2018.
- [5] T. Schlegl, T. Bretterkieber, S. Mühlbacher-Karrer, and H. Zangl, "Simulation of the leakage effect in capacitive sensing," *International Journal on Smart Sensing and Intelligent Systems*, vol. 7, no. 4, p. 1579 – 1594, Dec 2014.
- [6] Y. Ding, H. Zhang, and U. Thomas, "Capacitive proximity sensor skin for contactless material detection," in *2018 IEEE/RSJ International Conference on Intelligent Robots and Systems*, Oct 2018, to be published.